Exploring connections between global climate indices and African vegetation phenology

Molly E. Brown[1], Kirsten de Beurs[2], Anton Vrieling[3]

[1]Biospheric Sciences Branch, NASA Goddard Space Flight Center, Greenbelt, MD 20771, United States
[2]Virginia Polytechnic Institute and State University, Department of Geography, 115 Major Williams Hall, Blacksburg, VA 24061, United States
[3]Joint Research Centre of the European Commission, TP266, Via E. Fermi 2749, 21027 Ispra (VA), Italy

Abstract

Variations in agricultural production due to rainfall and temperature fluctuations are a primary cause of food insecurity on the continent in Africa. Agriculturally destructive droughts and floods are monitored from space using satellite remote sensing by organizations seeking to provide quantitative and predictive information about food security crises. Better knowledge on the relation between climate indices and food production may increase the use of these indices in famine early warning systems and climate outlook forums on the continent. Here we explore the relationship between phenology metrics derived from the 26 year AVHRR NDVI record and the North Atlantic Oscillation index (NAO), the Indian Ocean Dipole (IOD), the Pacific Decadal Oscillation (PDO), the Multivariate ENSO Index (MEI) and the Southern Oscillation Index (SOI). We explore spatial relationships between growing conditions as measured by the NDVI and the five climate indices in Eastern, Western and Southern Africa to determine the regions and periods when they have a significant impact. The focus is to provide a clear indication as to which climate index has the most impact on the three regions during the past quarter century. We found that the start of season and cumulative NDVI were significantly affected by variations in the climate indices. The particular climate index and the timing showing highest correlation depended heavily on the region examined. The research shows that climate indices can contribute to understanding growing season variability in Eastern, Western and Southern Africa.

1.0 Introduction

Satellite remote sensing has become a primary input to programs that monitor food production in Africa. In much of Africa, rainfed agriculture is a primary occupation and source of food for rural residents (Alberts and Mehta 2004; Breman 2003). Hundreds of millions of Africans rely on sufficient rainfall and moderate temperatures in order to produce enough food to feed their families (FAO 2006). Global trends in climate are increasingly impacting rainfall and temperature (Parry et al. 2007), which may ultimately reduce the ability of Africans to grow their own food (USAID 2007).

1

2 As population increases and food supplies become more constrained, the need to monitor
3 agricultural production even in the least productive regions will grow (Funk et al. 2008).
4 This highlights the need to understand the relationship between climate variability and
5 the indices that monitor local productivity. The amount of food produced locally often
6 interacts with global commodity prices to determine the price of food on the market,
7 affecting the ability of millions of poor urban and rural Africans to access food (Brown et
8 al. 2006). The stability of governments and regions often are disrupted when there is a
9 widespread lack of access and increasing hunger due to rising food prices (FEWS 2008;
10 Vasagar 2005).
11

12 Vegetation index data are often used by agencies monitoring agricultural conditions to
13 assess and predict agricultural production and identify periods of weather-related
14 production declines (Brown 2008b). Vegetation and rainfall data have become the basis
15 for operational monitoring of agricultural production, assessing variables such as the start
16 of season, growing season length and overall growing season productivity (Brown 2008a;
17 Brown and De Beurs 2008). Phenology metrics have a strong relationship with ultimate
18 food production, particularly those with sufficiently long records to capture local
19 variability (Funk and Budde 2008; Vrieling et al. 2008). Previous authors have used the
20 long term climate data record from the AVHRR instruments on the NOAA satellites as an
21 environmental observational record which may be directly related to climate variations
22 (Anyamba 1997; Verdin et al. 1999). Here we explore the relationship between
23 vegetation index data and five common climate indices to determine which most
24 influences local growing conditions in Sub-Saharan Africa.
25

26 Climate indices are used to reflect the essential elements of climate and its fluctuations
27 through time. ENSO (El Niño Southern Oscillation) is the best known index of climatic
28 variability, but others also express interannual climatic variability in Africa. Here we use
29 the North Atlantic Oscillation index (NAO), the Indian Ocean Dipole (IOD), the Pacific
30 Decadal Oscillation (PDO), the Multivariate ENSO Index (MEI) and the Southern
31 Oscillation Index (SOI). Each of these has been explored independently? in the literature
32 as to their impact on the African climate (Anyamba et al. 2001; Green and Hay 2002;
33 Jury et al. 1994; Rasmussen 1991; Verdin et al. 1999; Wang 2003). Strong negative SOI
34 anomalies are associated with an "El Niño" event (Cane et al. 1996) and strong positive
35 departures of the SOI are associated with "La Niña" conditions (Rasmusson and Wallace
36 1983). Warm ENSO events are characterized by above normal Sea Surface Temperatures
37 (SSTs) in the eastern Pacific and sometimes above normal SSTs in the western Indian
38 Ocean, as described by the IOD. Warm ENSO events, documented in the MEI, are
39 known to increase precipitation in some regions of Eastern Africa and result in droughts
40 in southern Africa (Glantz et al. 1991; Ropelewski and Halpert 1987).
41

42 By examining the spatial distribution and interaction of these effects, we can determine
43 which indices are most important in each region. This could provide guidance to model
44 developers and analysts working in the region. By conducting an analysis with many
45 climate indicators and multiple phenological metrics, we intend to cast a broad enough

1 net to provide guidance for data analysts who at present are focusing solely on one metric
2 in exclusion of others.
3
4 **2.0 Data**
5
6   **2.1 Normalized Difference Vegetation Index Data**
7 We used maximum value AVHRR NDVI composites (Holben 1986) from the NASA
8 Global Inventory Monitoring and Modeling Systems (GIMMS) group at NASA's
9 Biospheric Sciences Branch from July 1981 to December 2008 (Tucker et al. 2005). A
10 post-processing satellite drift correction has been applied to this dataset to further remove
11 artifacts due to orbital drift and changes in the sun-target-sensor geometry (Pinzon et al.
12 2005). The GIMMS operational dataset incorporates data from sensors aboard NOAA-7
13 through 14 with the data from the AVHRR on NOAA-16 and 17 using SPOT data as a
14 bridge for a by-pixel inter-calibration. Details of this calibration can be found in (Tucker
15 et al. 2005).
16
17   **2.2 Climate Indices**
18 We used five indices of global climate variations based on variations in atmospheric
19 pressure and sea surface temperatures from various regions. These are the North Atlantic
20 Oscillation index (NAO), the Indian Ocean Dipole (IOD), the Pacific Decadal Oscillation
21 (PDO), the Multivariate ENSO Index (MEI) and the Southern Oscillation Index (SOI).
22 We used the following indices:
23 - NAO: ftp://ftp.cpc.ncep.noaa.gov/wd52dg/data/indices/tele_index.nh
24 - IOD: http://www.jamstec.go.jp/frsgc/research/d1/iod/
25 - PDO: http://jisao.washington.edu/pdo/PDO.latest
26 - MEI: http://www.cdc.noaa.gov/ClimateIndices/
27 - SOI: http://www.cpc.ncep.noaa.gov/data/indices/soi
28 Figure 1 gives an overview of the variability of the indices over the past 26 years.

29 A mode of climate variability with extensive effects in the Northern Hemisphere, is the
30 Northern Annular Mode (NAM; (Thompson and Wallace 2001)), which also goes by the
31 name of the North Atlantic Oscillation (NAO; (Hurrell 1995)). The North Atlantic
32 Oscillation (NAO) index is typically measured through variations in the normal pattern of
33 lower atmospheric pressure over Iceland and higher pressure near the Azores and Iberian
34 Peninsula (Jones et al. 1997). A positive NAO index refers to an increased difference in
35 pressure between these two regions and thus stronger westerly winds. This corresponds to
36 a stronger storm track across the Atlantic from Western Africa. The negative mode of the
37 NAO—when there is less difference than usual in pressure across the two regions—
38 features a weakened Atlantic storm track. The NAO trended toward more positive values
39 from the 1960s to the mid-1990s, but has since returned to more normal values (UCAR
40 2009).

41 The Indian Ocean Dipole (IOD) is an interannual (year-to-year) climate pattern across the
42 tropical Indian Ocean first identified in 1999 (Saji et al. 1999). In the positive phase of
43 the IOD, trade winds are stronger than usual and cooler-than-average sea-surface
44 temperatures are prevalent across the eastern tropical Indian Ocean, near Indonesia and

Australia. To the west, near Madagascar, waters are warmer than average and convection is intensified, thus causing heavy rainfall in Eastern parts of Africa. These patterns are reversed during the IOD's negative phase(UCAR 2009).

The Pacific Decadal Oscillation (PDO) is a multidecadal pattern of climate variability centered across the North Pacific Ocean (Mantua et al. 1997). During the positive (warm) phase of the PDO, sea-surface temperatures tend to be above average along the west coast of North America and in the eastern tropical Pacific; while across the central North Pacific they are cooler than average. The opposite patterns occur during the negative (cool) phase. The PDO may be related to ENSO, but differs mainly because the timescale for the PDO is much longer (several decades) and because the PDO more clearly involves the extratropical Pacific and the Aleutian low pressure system (UCAR 2009). The impact of the PDO on the climate of Africa during the past few decades is unclear, although studies suggest a correlation with rainfall in Eastern and Southern Africa (Mantua and Hare, 2002).

The Multivariate ENSO Index (MEI) is a measure of the comparative strength of El Nino Southern Oscillation (ENSO) events (Wolter and Timlin 1998). It is derived by combining several different indices that separately measure weather variables in the tropical Pacific, such as sea-surface temperature, sea-level pressure (SOI), surface winds, surface air temperature, cloudiness, precipitation, and other variables (UCAR 2009).

Finally, the Southern Oscillation Index (SOI) is a measure that represents the strength of the Southern Oscillation in the Pacific Ocean sea surface temperatures and pressures (Reynolds et al. 2002). An SOI is typically created by comparing the sea-level pressures measured at Tahiti (in the South Pacific) to those at Darwin, Australia, and listing the anomalies (the departures from average). During El Niño, pressures tend to be below normal at Tahiti and above normal at Darwin, producing a negative SOI. The opposite is true during La Niña (UCAR 2009). Research has shown that negative SOI (El Niño) is associated with dry weather and a positive SOI (La Niña) related to wet weather conditions in Southernern Africa. These variations are linked to variations in malaria incidence (Mabaso et al. 2009).

3.0 Methods

The NDVI data were temporally filtered and phenology parameters were extracted in order to estimate the potential impact of the climate indices on growing season variability in the region and consequently on food production. Temporal filtering was performed to reduce any remaining cloud effect in the NDVI data by means of an iterative Savitzky-Golay filter (Chen et al. 2004). Three regions were analyzed, Eastern Africa, Western Africa and Southern Africa (Figure 2).

To extract phenology variables, we used the percent threshold or mid-point NDVI method proposed by (White et al. 1997). The onset and conclusion of the growing season are estimated using NDVI curves, extracting for each pixel and year the start of season (SOS), and end of season (EOS) as the timing of the crossing of the 50% point of the

NDVI curve in upward or downward direction respectively. Since the African growing seasons do not everywhere fall within one calendar year, we determined SOS and EOS based on two different time periods both incorporating 1.5 years of data: Cycle 1: October Year 1 – March Year 3 Cycle 2: April Year 2 – October Year 3 (Figure 3). These time frames allow for the estimation of growing seasons in both the Northern Hemispheric and the Southern Hemispheric parts of Africa. In addition, it allows for the detection of double cropped regions such as can be found in Eastern Africa.

A total of five phenology indicators were considered for this analysis. Besides SOS and EOS, we determined the length of season (LOS), the maximum NDVI of the season (maxNDVI), and the cumulated NDVI over the season (cumNDVI). The extraction of these parameters is straightforward based on SOS, EOS, and the filtered time series (Figure 4). The length of season (LOS) parameter is calculated as LOS=EOS−SOS. We defined that LOS should be at least more than a month to be valid, and before calculating other indicators.

The five phenology indicators described above were correlated to the five climate indices NAO, PDO, MEI, IOD and SOI. To reduce noise and increase the signal for each climate index, we aggregated the monthly data into four seasons to determine the correlation with the vegetation index phenology indicators: DJF – December, January, February; MAM – March, April, May; JJA – June, July, August; and SON – September, October, November. These were then correlated with the annual phenology indicators over two-year cycles to capture the effect of the index during each season on the annual phenology metrics for the same year as the index aggregation and on the next year, enabling the capturing of as broad a range of impact as possible of each climate indicator.

We used the non-parametric Spearman rank correlation to determine the strength of the association between the climate indices and the phenological metrics (Lehman and D'Abrera 1975). The Spearman rank correlation coefficient is based on the ranked values of the variables rather than on the values themselves as in the common Pearson correlation coefficient. The Spearman correlation makes no assumption with respect to the underlying frequency of the variables and does not presume the variables to be linearly related. Since theoretical studies have shown that the interaction between vegetation and atmosphere is non-linear, e.g. (Bonan 2002), these are important considerations. If the interaction were indeed non-linear, the Pearson correlation coefficient or simple linear regression could either over or under estimate the strength of the relation (de Beurs and Henebry 2008).

The results were simplified into the three regions of interest where the NDVI has the strongest correlation to production in semi-arid zones: Eastern, Southern and Western Africa. We calculated the total number of pixels with positive and with negative trend correlations in the regions as well as the percent of significant trends within each category (Figure 5). In this way we were able to characterize the overall impact of a particular climate index for a region and therefore its importance on growing conditions during the past 26 years.

When a statistical test (such as the Spearman rank correlation test) is run a large number of times, a certain number of false positive results is expected. The rate of false positives allowed for the test statistic is determined by the α-level. For example, if we set the α-level at 0.10 and we apply a statistical test 1000 times, we could expect to find about 100 rejections of the null hypothesis while there is in fact no correlation (de Beurs and Henebry 2008). Here we analyze the correlation results by region. By setting our α-level at 0.10, we argue that a geographic region with more than the expected 10% significant pixels, can be considered to have revealed significant correlation. We report our findings using the percent of the geographic area with either positive or negative significant correlations between SOS and CumNDVI and the climate index in a season in the interest of space. The influence of the climate indicator is thus estimated using vegetation index data from the past 25 years, estimating its impact on the local climate and agricultural production across a broad region. In the next section we will present the key findings.

4.0 Results

4.1 Regional Results

In Southern Africa we found that all climate indices were influential on one or more of the phenology parameters at some period of the year. As other authors have found, Southern Africa is sensitive to both the pacific and ENSO effects (Eastman et al. 1996; Nicholson 2003; Ropelewski and Halpert 1986). The end of the growing season parameter was particularly sensitive to the PDO, MEI, NAO and IOD, although this parameter may be less robust than that of SOS or the cumulative NDVI (detailed below).

Eastern Africa, with results from both cycle 1 and cycle 2 analyses, the SOS shows a sensitivity to the PDO indicator during the MAM and DJF periods, with less impact at other times of the year. The MEI index also has a very strong influence on SOS and CumNDVI in the region, particularly in SON and DJF. NAO and IOD have only a small influence in the region.

In Western Africa, PDO was the most important index, influencing both the start and length of the growing season in the central area compromising northern Nigeria, Ghana and the Ivory Coast. The two ENSO indicators MEI and SOI also have their impact in the growing season, but the effect is less strong then the PDO. The NAO during SON had a strong negative influence on the start of season (e.g. 61% of Western Africa revealed a positive correlation between SOS and NAO_SON0, which is the September-October-November period preceding the observed growing season, Table 1), end of season and the season length (Fontaine et al. 1998). The IOD did not seem to have much influence in the region.

4.2 Start of Season Results

SOS is an important measure of the ultimate success of the growing season in many rainfed agricultural systems (Brown and De Beurs 2008; Funk and Budde 2008). Delayed starts shorten the growing season in some regions, directly reducing the yield

because generally the rains end before crops are fully mature. In other regions, variations in global climate indices are related to early starts, which may provide a longer season with more rain.

Table 1 reports the impact of each climatic index on SOS from eight different three month groups. The climate indices start three 3-month periods before the growing season e.g. for Southern Africa and the second cycle of Eastern Africa the growing season typically starts in the period September-October-November (the *belg* rains in Ethiopia). NAO-DJF1 is the NAO index of December-January-February in the year 1, thus three 3-month periods before average SOS in Southern and Eastern Africa. The growing season in Western Africa and the first cycle of Eastern Africa typically starts in the period March-April-May of year 1 (MAM1). The correlations are reported for the indices starting three 3-month periods earlier (e.g. June-July-August of year 0).

The results show that in the first growing cycle in Eastern Africa, the March-April-May Pacific Decadal Oscillation (PDO_MAM1) affects the start of the growing season in 72% of the region with a positive correlation, meaning when the PDO is elevated, the growing season will start later in 72% of the region. This correlation is significant in 32% of the region. It is interesting to see that the two preceding periods (PDO_SON0 and PDO_DJF1) also reveal between 70-72% positive correlation between SOS and PDO. However, the correlation is significant in a lower percentage of pixels (18 and 24% respectively).

Figure 5 shows the spatial distribution of the correlation between SOS and PDO_MAM1 with their corresponding p-values. A large area of positive significant correlation can be seen in Eastern Ethiopia as well as on the border between Ethiopia and Sudan, the site of an ongoing and severe drought. There is another area with significant positive correlation in central Kenya. It is interesting to see north-south patch of significant negative correlation in the higher laying areas of central Ethiopia. Eastern Africa also reveals positive correlation in 72% of the region between the Multivariate ENSO Index (MEI) during the DJF period (MEI_DJF1) and the start of the growing season in Eastern Africa. Again, the two preceding periods (MEI_JJA0 and MEI_SON0) reveal similar positive correlation. This time the percentage of significant correlations is about 18% for all three time periods. Correlations with SOI are reversed, with 75% negative correlation between SOS and SOI_JJA0.

Southern African phenology metrics are influenced by from all five climate metrics. The SOI index shows positive correlations with changes in SOS, and NAO, PDO, and IOD reveal negative correlations with the start of season (Table 1). MEI reveals both positive and negative correlations, although at different timings. Figure 6A and 6B shows the impact on the start of the growing season in Southern Africa of the Multivariate ENSO Index from March-April-May (MAM-1). This is two periods before average SOS in Southern Africa which falls between September and November. The region reveals positive correlation in 71% of the pixels, with 20% of the pixels being significant.

Figure 6 C and D show the correlation between IOD from June-July-August on the start of season (SOS) in Southern Africa. This is one period before the season starts in Southern Africa. In this case 71% of the region reveals positive correlation (19% is significant). Note the spatial pattern of the significance, with strong correlation and significance in the dryland regions of central Mozambique and eastern Zimbabwe, regions with fairly marginal agricultural productivity but with high variability from year to year. Also, the border area between Namibia, Botswana and South Africa reveals a region of with IOD significant negative correlation.

In Western Africa, the correlation patterns are generally less uniform, resulting in a mixture of positive and negative correlations. As a result, the regional percentage of correlation that is either positive or negative is lower. The Pacific Decadal Oscillation (PDO_DJF1) reveals one of the few significant positive correlations with the SOS (percentage positive is 0.66), as is seen in Table 1 and in Figure 7. The correlation between the December-January-February values of the PDO on SOS in the northern parts of Ivory Coast, Nigeria and central Guinea Conakry mean that when the PDO is elevated, the start of season is later.

4.3 Cumulative NDVI results

Cumulative NDVI has long been a parameter which has been used to correspond to growing period, agricultural productivity, changes in landscape pattern and other parameters (Chen et al. 2000; Chuvieco 1999; Ji and Peters 2003; Rasmussen 1998). Figure 8A shows the correlation between the MEI from September-October-November (MEI_SON1) on cumulative NDVI from Cycle 2 (long season rains) in Eastern Africa (75% positive correlation). Figure 8B shows the significance (p-value, 22% significant). This period coincides with SOS for the second cycle in Eastern Africa. The next two 3-month period, which fall within the growing season, also reveal high percentages of significant positive correlations. Figure 8C shows the correlation between the SOI from June-July-August (SOI_JJA1) on cumulative NDVI and Figure 8D the significance of the correlation.   SOI values in June-July-August (SOI_JJA1) show significant (75% of the pixels are negatively correlated, 31% of the correlations are significant) and strong correlations with cumulative NDVI in the eastern and central Ethiopia and the rangeland areas of Kenya (Figure 8). Again, the two preceding periods which still fall within the growing season, show similar significant correlations. These spatial patterns are very interesting given the long term drought seen in these regions during the past few years.

Table 2 highlights the strong relationship between PDO and the cumulative NDVI in Western Africa before the actual start of the growing season. PDO reveals significant negative correlations with cumulative NDVI in the four periods JJA0, SON0, DJF1 and MAM1. The growing season typically starts during the period MAM1. The regions where strong PDO relationships are seen for the cumulative NDVI are similar to those seen for SOS (Figure 7), which is to be expected since a delayed start of season will result in a lower cumulative NDVI.

4.4 Results by region, with a focus on the Pacific Decadal Oscillation

Figure 9 shows plots for each region that summarize the effect of four parameters on SOS in each region. For clarity we have omitted SOI, which shows a similar although opposite pattern as MEI. The figures show the percent of the region with negative correlations between the climate index and SOS. Negative correlations denote an earlier SOS for a higher index value. Only the values for the second cycle of Eastern Africa are plotted. Note the strong negative correlations between SOS and PDO in both Eastern and Southern Africa, more than 70% of the region affected. The area that the PDO influences grows through time, with stronger correlations during the growing season than in the dry season. In both Southern and Eastern Africa the climate indices appear to become fairly similar around the time of SOS (indicated by the vertical line).

Figure 10 shows the results for all three regions divided by climatic index. Figure 10A shows the results for the PDO and are particularly interesting. In both Southern and Western Africa, the index is revealing strong correlations, with high negative correlation in Western Africa and high positive (thus low negative) correlation in Southern Africa. The impact of the PDO on the climate of Africa during the past few decades is unclear, although Rouault (2002) examined the association between the PDO and South African rainfall and noted that the warm (cool) phase of the interdecadal variability in the Pacific and Indian Ocean is associated with decreased (increased) rainfall over South Africa (Reason and Rouault 2002). Figure 10B shows the MEI and 10C the NAO results. The MEI has the strongest seasonal effect, increasing during the short and long seasons of Eastern Africa and declining since.

5.0 Discussion

The results of this paper highlight climate-vegetation relationships that could be very valuable for the analysis of seasonal variation in the climate in Africa. The relationships we find here are evidence of recurring and persistent, large-scale pattern of pressure and circulation anomalies that span vast geographical areas. Here we show that seasonal phenological patterns as derived from the 26 year vegetation index record can be used to estimate the importance or lack of importance of the various indices in Western, Eastern and Southern Africa.

The GIMMS NDVI dataset is not perfect as a source of information on agricultural productivity or characteristics. Here we transform the bimonthly dataset into five phenological parameters, but these are not equal in stability. Previous research and extensive use of GIMMS NDVI and phenology metrics in Africa through the USAID's Famine Early Warning Systems Network has shown that the start of season and cumulative NDVI are the most stable and reliable parameters, with the longest record of use and publications in Africa (Brown 2008b). The end of season parameter is influenced by land cover type and the cumulative NDVI could be affected by the degree of cloudiness during the peak of the rainy season and the calibration between sensors through time (Tucker et al. 2005). However, by using phenological parameters, we are able to move significantly closer to understanding the impact of climate variability on agriculture.

SOS is particularly important for determining yields in a given season, since in many semi-arid areas, the length of the growing season is an important determinant of yield. If the season begins late, the likelihood of average yields declines significantly (FEWS 1992; Groten and Ocatre 2002; Verdin et al. 2000). Thus negative correlations (implying a later start for lower index values) with SOS over the 25 year NDVI record is an important estimate of the impact of the climate indicator on overall agricultural productivity in that season because in semi-arid zones, a delayed start results in reduced yields. Variations in climate indices can then be used to estimate future changes in growing season length, start and strength based on this research.

In Eastern Africa, we found high negative correlations between SOS during the second cycle and MEI, particularly in the semi-arid pastoral zone of eastern Ethiopia, Somalia and northeastern Kenya (see Figure 8). This region has been experiencing a multi-year drought during the past decade which has resulted in failed harvests, water shortages and deteriorating rangeland conditions (FEWSNET 2006; Funk et al. 2005). The effect of the global climate system on this region where there are millions of food insecure and hungry agriculturalists and pastoralists has been a topic of much recent research (Funk et al. 2008)

In Western Africa, we have identified a similar relationship between the Atlantic multidecadal variability as represented by the NAO and Sahel rainfall as was documented in (Zhang and Delworth 2006). Exploration of these relationships in the context of prediction and estimation of rainfall in the region is warranted, and may result in improved seasonal prediction in, for example, the regional climate outlook forums held before the main growing season every year (Brown et al. 2007).

Future research will focus on the forecasting potential of climatic indices for phenological metrics and thus crop production. Future steps would be to assess the simultaneous impact of multiple climatic indices on the observed phenology events. Impacts of different indices could be additive, potentially resulting in increased explanatory power. In addition, our figures show that high correlation exists in sub-regions of Western, Eastern and Southern Africa. Thus, detailed impact studies in sub-regions may be useful as well.

6.0 Conclusions

Given the agricultural nature of most economies on the African continent, agricultural production continues to be a critical determinant of both food security and economic growth (Funk and Brown 2009). In this paper, we explore the relationship between climate indices and phenology metrics derived from NDVI data to determine how influential each metric is on the growing season. Crop phenological parameters, such as the start and end of the growing season, the total length of the growing season, and the rate of greening and senescence are important for planning crop management and crop diversification and intensification. Because these crop parameters are sensitive to climate variability, understanding which climate indices are most influential and affect variation

1   in these metrics from one year to the next can improve seasonal analysis and agriculture
2   planning across the continent.
3
4   We found that the start of season and cumulative NDVI were significantly affected by
5   variations in the climate indices in the three regions examined. Eastern Africa that has
6   been experiencing drought in recent years is particularly sensitive to PDO variations in
7   March-April-May. In Western Africa, we have identified a relationship between NAO
8   and Sahel rainfall as expressed by vegetation. The growing season in Southern African is
9   sensitive to variations in the ENSO metrics SOI and MEI, as well as PDO. Research that
10 uses current climate indices to estimate variability in the next growing season for each
11 region is the subject of future research, as this will enhance the utility of this research for
12 many users of remote sensing in the region.

Table 1. Start of Season correlation and significance for five metrics and three regions.   %+ = the percentage of pixels with positive correlation. %+ sign = the percentage of pixels with positive correlation that are significant. %- = the percentage of pixels with negative correlation. %-sign = percentage of pixels with negative correlation that are significant. Eastern Africa results are from Cycle 1 results, derived from the January to December period.

Index	*Southern Africa*				*Eastern Africa*				*Western Africa*				
Period	%+	%+ sig.	%-	%-sig.	%+	%+ sig.	%-	%-sig.	%+	%+ sig.	%-	%-sig.	**Period**
	← ← ← ← ← ← ← ← ←				→ → → → → → → → → → →				→ → → → → → → → → → →				
NAO_DJF1	0.51	0.09	0.49	0.08	0.43	0.10	0.57	0.10	0.34	0.05	0.66	0.13	NAO_JJA0
NAO_MAM1	0.33	0.04	0.67	0.13	0.44	0.05	0.56	0.10	0.61	0.14	0.39	0.08	NAO_SON0
NAO_JJA1	0.69	0.16	0.31	0.04	0.59	0.09	0.41	0.06	0.43	0.07	0.57	0.11	NAO_DJF1
NAO_SON1	0.29	0.09	0.71	0.23	0.44	0.06	0.56	0.08	0.45	0.05	0.55	0.08	NAO_MAM1
NAO_DJF2	0.51	0.08	0.49	0.07	0.34	0.07	0.66	0.16	0.53	0.07	0.47	0.06	NAO_JJA1
NAO_MAM2	0.49	0.11	0.51	0.09	0.40	0.05	0.60	0.10	0.39	0.06	0.61	0.13	NAO_SON1
NAO_JJA2	0.53	0.08	0.47	0.07	0.50	0.08	0.50	0.08	0.52	0.09	0.48	0.07	NAO_DJF2
NAO_SON2	0.49	0.11	0.51	0.13	0.31	0.04	0.69	0.16	0.57	0.15	0.43	0.14	NAO_MAM2
PDO_DJF1	0.36	0.05	0.64	0.11	0.56	0.08	0.44	0.09	0.49	0.06	0.51	0.07	PDO_JJA0
PDO_MAM1	0.45	0.06	0.55	0.10	0.72	0.18	0.28	0.04	0.59	0.10	0.41	0.05	PDO_SON0
PDO_JJA1	0.60	0.10	0.40	0.06	0.70	0.24	0.30	0.10	**0.66**	**0.17**	0.34	0.05	PDO_DJF1
PDO_SON1	0.32	0.04	0.68	0.15	**0.72**	**0.32**	0.28	0.11	0.57	0.13	0.43	0.06	PDO_MAM1
PDO_DJF2	0.24	0.03	0.76	0.18	0.56	0.13	0.44	0.09	0.48	0.07	0.52	0.09	PDO_JJA1
PDO_MAM2	0.28	0.04	0.72	0.14	0.56	0.14	0.44	0.08	0.43	0.07	0.57	0.11	PDO_SON1
PDO_JJA2	0.40	0.06	0.60	0.08	0.61	0.16	0.38	0.13	0.53	0.10	0.47	0.07	PDO_DJF2
PDO_SON2	0.43	0.09	0.57	0.10	0.50	0.10	0.50	0.11	0.40	0.06	0.60	0.10	PDO_MAM2
MEI_DJF1	0.67	0.14	0.33	0.05	0.73	0.18	0.27	0.04	0.55	0.07	0.45	0.05	MEI_JJA0
MEI_MAM1	**0.71**	**0.20**	0.29	0.05	0.72	0.17	0.28	0.04	0.61	0.12	0.39	0.08	MEI_SON0
MEI_JJA1	0.38	0.08	0.62	0.15	**0.72**	**0.18**	0.28	0.04	0.59	0.13	0.41	0.08	MEI_DJF1
MEI_SON1	0.27	0.06	**0.73**	**0.20**	0.60	0.14	0.40	0.09	0.50	0.12	0.50	0.13	MEI_MAM1
MEI_DJF2	0.29	0.07	0.71	0.20	0.57	0.14	0.43	0.08	0.38	0.11	0.62	0.17	MEI_JJA1
MEI_MAM2	0.38	0.08	0.62	0.15	0.52	0.12	0.48	0.09	0.36	0.07	0.64	0.14	MEI_SON1
MEI_JJA2	0.43	0.11	0.57	0.11	0.44	0.08	0.56	0.11	0.35	0.08	0.65	0.14	MEI_DJF2
MEI_SON2	0.50	0.10	0.50	0.08	0.32	0.06	0.68	0.19	0.25	0.04	0.75	0.22	MEI_MAM2

|													
IOD_DJF1	0.52	0.08	0.48	0.07	0.73	0.17	0.27	0.04	0.60	0.13	0.40	0.05	IOD_JJA0
IOD_MAM1	0.39	0.08	0.61	0.17	0.75	0.16	0.25	0.03	0.60	0.14	0.40	0.08	IOD_SON0
IOD_JJA1	0.29	0.05	**0.71**	**0.19**	0.63	0.12	0.37	0.05	0.64	0.10	0.36	0.05	IOD_DJF1
IOD_SON1	0.32	0.05	0.68	0.16	0.60	0.11	0.40	0.05	0.45	0.08	0.55	0.10	IOD_MAM1
IOD_DJF2	0.43	0.06	0.57	0.09	0.60	0.11	0.40	0.06	0.47	0.06	0.53	0.11	IOD_JJA1
IOD_MAM2	0.54	0.07	0.46	0.06	0.52	0.08	0.48	0.07	0.52	0.07	0.48	0.08	IOD_SON1
IOD_JJA2	0.43	0.07	0.57	0.08	0.47	0.07	0.53	0.09	0.64	0.13	0.36	0.06	IOD_DJF2
IOD_SON2	0.49	0.07	0.51	0.06	0.36	0.04	0.64	0.11	0.53	0.09	0.47	0.08	IOD_MAM2
SOI_DJF1	0.32	0.05	0.68	0.15	0.25	0.04	0.75	0.17	0.35	0.04	0.65	0.12	SOI_JJA0
SOI_MAM1	0.40	0.07	0.60	0.15	0.30	0.06	0.70	0.17	0.44	0.08	0.56	0.11	SOI_SON0
SOI_JJA1	0.69	0.17	0.31	0.05	0.34	0.06	0.66	0.15	0.36	0.07	0.64	0.14	SOI_DJF1
SOI_SON1	0.69	0.17	0.31	0.06	0.39	0.09	0.61	0.19	0.54	0.15	0.46	0.12	SOI_MAM1
SOI_DJF2	0.74	0.22	0.26	0.05	0.39	0.06	0.61	0.12	0.61	0.15	0.39	0.07	SOI_JJA1
SOI_MAM2	0.62	0.17	0.38	0.09	0.59	0.11	0.40	0.07	**0.68**	**0.17**	0.32	0.08	SOI_SON1
SOI_JJA2	0.51	0.07	0.49	0.10	0.62	0.14	0.38	0.07	0.69	0.15	0.31	0.04	SOI_DJF2
SOI_SON2	0.44	0.07	0.56	0.13	0.70	0.16	0.30	0.07	0.73	0.23	0.27	0.09	SOI_MAM2

Table 2. Cumulative NDVI correlation and significance for five metrics and three regions. %+ = the percentage of pixels with positive correlation. %+ sign = the percentage of pixels with positive correlation that are significant. %- = the percentage of pixels with negative correlation. %-sign = percentage of pixels with negative correlation that are significant. The Western Africa percentages use the index labels on the right.

Index Period	Southern Africa				Eastern Africa				Western Africa				Period
	%+	%+ sig.	%-	%-sig.	%+	%+ sig.	%-	%-sig.	%+	%+ sig.	%-	%-sig.	
	← ← ← ←← ← ← ←←←				← ← ← ←← ← ← ←←←				→→→→→→→→→→→→				
NAO_DJF1	0.44	0.08	0.56	0.11	0.40	0.06	0.60	0.12	0.37	0.07	0.63	0.14	NAO_JJA0
NAO_MAM1	0.45	0.07	0.55	0.09	0.70	0.17	0.30	0.05	0.36	0.05	0.64	0.11	NAO_SON0
NAO_JJA1	0.54	0.10	0.46	0.07	0.48	0.08	0.52	0.08	0.52	0.06	0.48	0.06	NAO_DJF1
NAO_SON1	0.38	0.06	0.62	0.15	0.48	0.07	0.52	0.07	0.54	0.08	0.46	0.06	NAO_MAM1
NAO_DJF2	0.45	0.07	0.55	0.11	0.36	0.04	0.64	0.12	0.41	0.06	0.59	0.07	NAO_JJA1
NAO_MAM2	0.41	0.07	0.59	0.11	0.31	0.05	0.69	0.22	0.36	0.07	0.64	0.13	NAO_SON1
NAO_JJA2	0.27	0.04	0.73	0.18	0.28	0.04	0.72	0.15	0.47	0.09	0.53	0.08	NAO_DJF2
NAO_SON2	0.58	0.16	0.42	0.11	0.50	0.09	0.50	0.09	0.43	0.11	0.57	0.15	NAO_MAM2
PDO_DJF1	0.56	0.12	0.44	0.09	0.44	0.07	0.56	0.10	0.27	0.06	0.73	0.21	PDO_JJA0
PDO_MAM1	0.52	0.08	0.48	0.08	0.40	0.09	0.60	0.13	0.30	0.05	0.70	0.17	PDO_SON0
PDO_JJA1	0.60	0.09	0.40	0.05	0.62	0.10	0.38	0.05	0.30	0.05	**0.70**	**0.18**	PDO_DJF1
PDO_SON1	0.33	0.05	0.67	0.12	0.65	0.12	0.35	0.05	0.30	0.04	0.70	0.15	PDO_MAM1
PDO_DJF2	0.42	0.07	0.58	0.10	0.59	0.10	0.41	0.06	0.39	0.06	0.61	0.08	PDO_JJA1
PDO_MAM2	0.39	0.06	0.61	0.11	0.59	0.11	0.41	0.07	0.35	0.12	0.65	0.25	PDO_SON1
PDO_JJA2	0.33	0.06	0.67	0.14	0.50	0.07	0.50	0.08	0.33	0.10	0.67	0.20	PDO_DJF2
PDO_SON2	0.44	0.07	0.56	0.09	0.45	0.08	0.55	0.09	0.38	0.07	0.62	0.10	PDO_MAM2
MEI_DJF1	0.42	0.06	0.58	0.10	0.28	0.04	**0.72**	**0.15**	0.37	0.07	0.63	0.12	MEI_JJA0
MEI_MAM1	0.43	0.05	0.57	0.09	0.37	0.06	0.63	0.12	0.29	0.07	0.71	0.16	MEI_SON0
MEI_JJA1	0.35	0.08	0.65	0.17	0.66	0.13	0.34	0.06	0.33	0.06	0.67	0.14	MEI_DJF1
MEI_SON1	0.33	0.07	0.67	0.18	**0.75**	**0.22**	0.25	0.05	0.37	0.05	0.63	0.14	MEI_MAM1
MEI_DJF2	0.33	0.08	0.67	0.21	0.74	0.25	0.26	0.06	0.44	0.07	0.56	0.12	MEI_JJA1
MEI_MAM2	0.30	0.08	0.70	0.25	0.72	0.24	0.28	0.07	0.40	0.06	0.60	0.10	MEI_SON1
MEI_JJA2	0.33	0.06	0.67	0.18	0.51	0.08	0.49	0.08	0.47	0.08	0.53	0.09	MEI_DJF2
MEI_SON2	0.36	0.05	0.64	0.13	0.32	0.05	0.68	0.15	0.53	0.11	0.47	0.10	MEI_MAM2

IOD_DJF1	0.33	0.05	0.67	0.13	0.42	0.06	0.58	0.10	0.47	0.07	0.53	0.09	IOD_JJA0
IOD_MAM1	0.39	0.06	0.61	0.11	0.49	0.08	0.51	0.08	0.37	0.05	0.63	0.12	IOD_SON0
IOD_JJA1	0.35	0.05	0.65	0.12	0.57	0.10	0.43	0.08	0.41	0.05	0.59	0.08	IOD_DJF1
IOD_SON1	0.44	0.07	0.56	0.10	0.72	0.20	0.28	0.05	0.58	0.15	0.42	0.09	IOD_MAM1
IOD_DJF2	0.54	0.10	0.46	0.08	0.69	0.14	0.31	0.06	0.53	0.08	0.47	0.05	IOD_JJA1
IOD_MAM2	0.52	0.09	0.48	0.08	0.52	0.09	0.48	0.07	0.50	0.07	0.50	0.05	IOD_SON1
IOD_JJA2	0.52	0.07	0.48	0.07	0.40	0.05	0.60	0.09	0.61	0.11	0.39	0.04	IOD_DJF2
IOD_SON2	0.47	0.08	0.53	0.09	0.35	0.05	0.65	0.13	0.64	0.17	0.36	0.06	IOD_MAM2
SOI_DJF1	0.54	0.08	0.46	0.06	0.73	0.20	0.27	0.05	0.68	0.12	0.32	0.04	SOI_JJA0
SOI_MAM1	0.58	0.10	0.42	0.07	0.58	0.08	0.42	0.06	0.65	0.12	0.35	0.07	SOI_SON0
SOI_JJA1	0.48	0.08	0.52	0.11	0.25	0.05	**0.75**	**0.31**	0.73	0.15	0.27	0.04	SOI_DJF1
SOI_SON1	0.68	0.20	0.32	0.07	0.28	0.06	0.72	0.23	0.54	0.14	0.46	0.12	SOI_MAM1
SOI_DJF2	0.67	0.21	0.33	0.08	0.22	0.06	0.78	0.29	0.46	0.11	0.54	0.11	SOI_JJA1
SOI_MAM2	0.75	0.28	0.25	0.07	0.34	0.07	0.66	0.14	0.57	0.10	0.43	0.08	SOI_SON1
SOI_JJA2	0.66	0.15	0.34	0.06	0.75	0.18	0.25	0.04	0.56	0.09	0.44	0.07	SOI_DJF2
SOI_SON2	0.65	0.13	0.35	0.05	0.67	0.18	0.33	0.06	0.52	0.12	0.48	0.11	SOI_MAM2
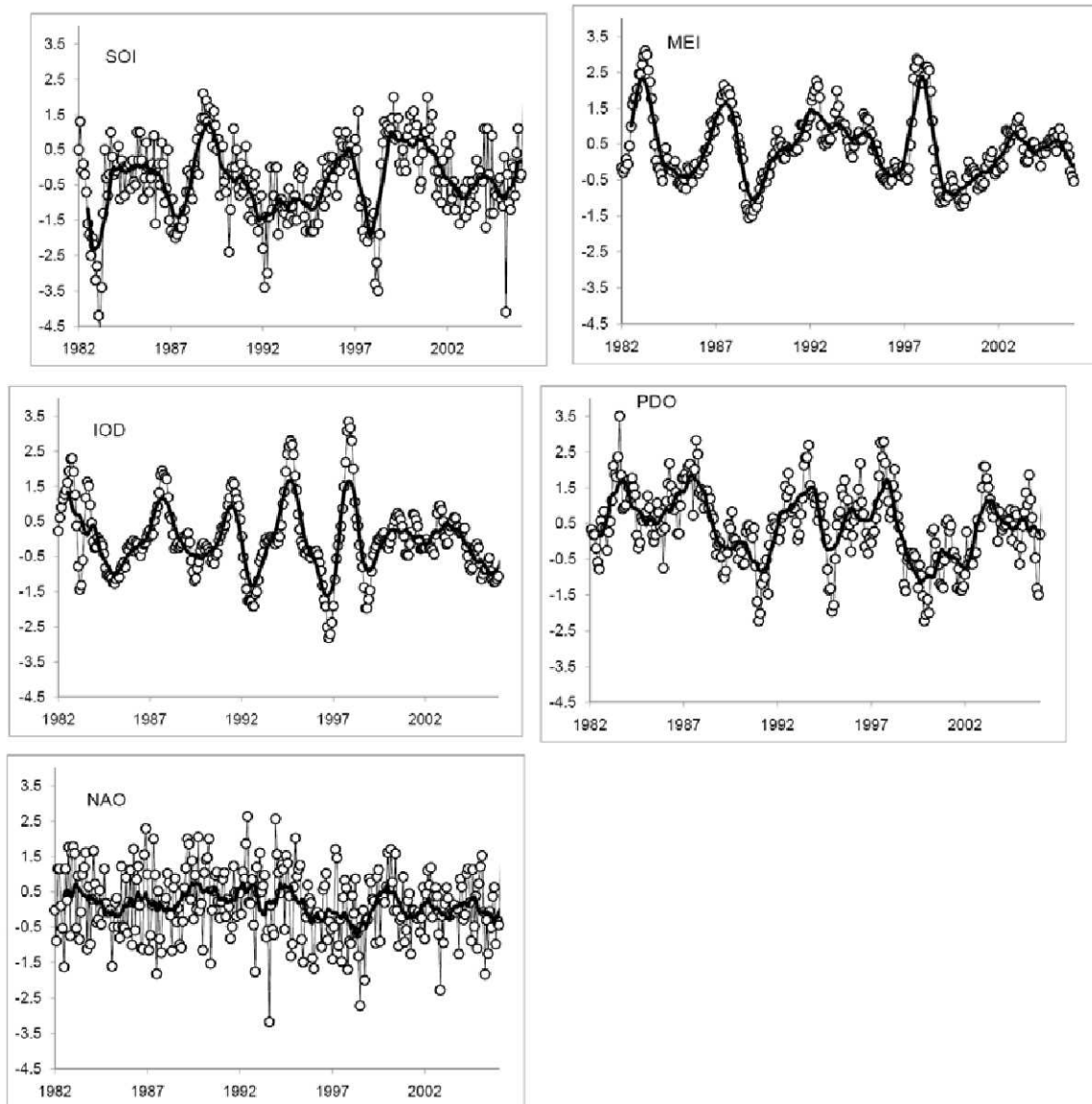
Figure 1. Monthly SOI, MEI, IOD, PDO and NAO indices from 1982-2007 with a 12 month trend line plotted. In this paper, we aggregate the monthly indices into seasonal averages to correlate with phenology metrics.
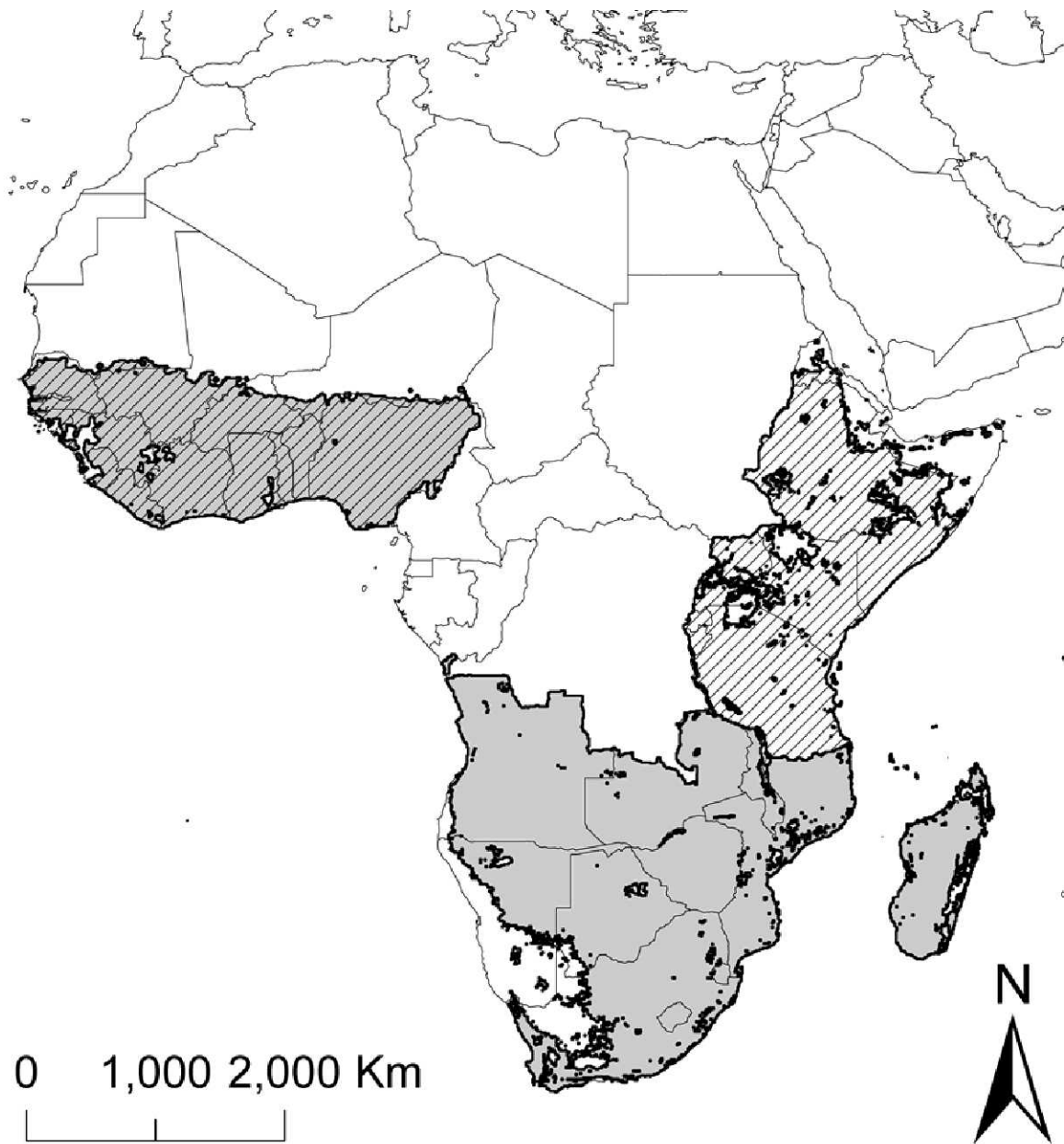
Figure 2. Map with regions addressed in this study. The gaps occur because a mask was applied eliminating all pixels with NDVI <0.2 or >0.7 or where the coefficient of variation of NDVI was <0.1.
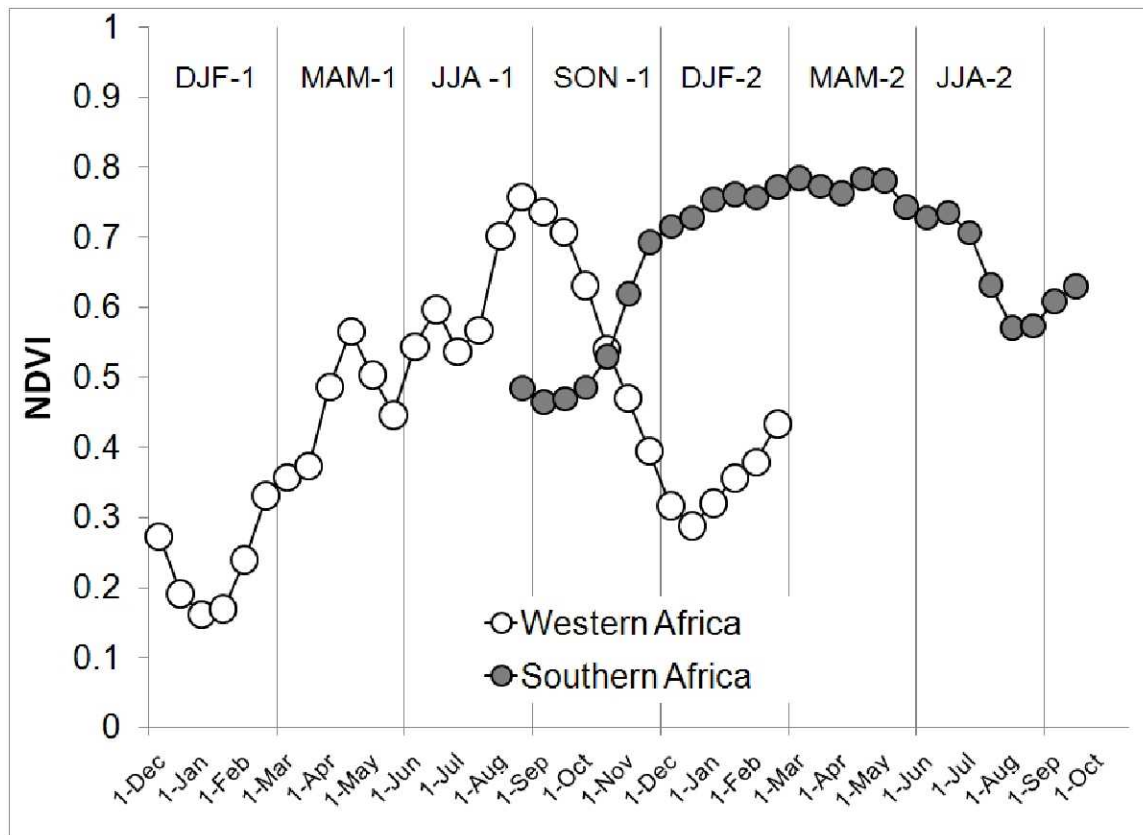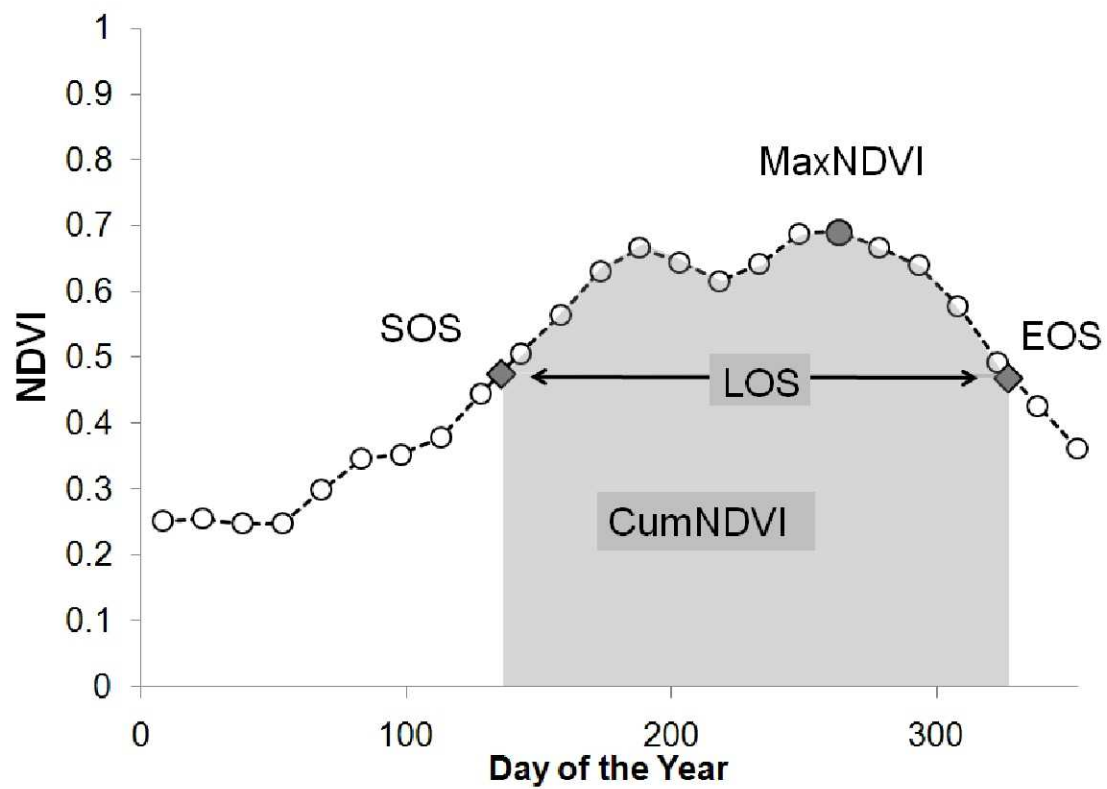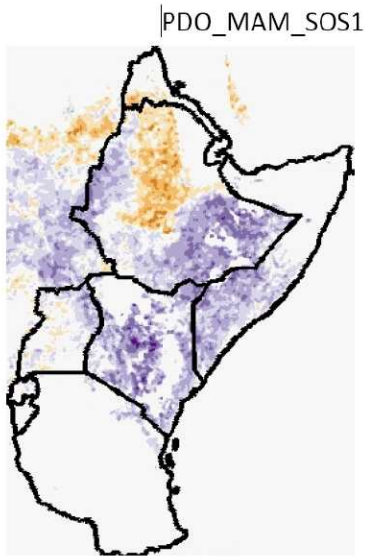
Figure 3. Two NDVI curves from Western and Southern Africa showing the two cycles of analysis, each a year and a half long: Cycle 1: October Year 1 – March Year 3, which captures summer rainy seasons which occur north of the equator, and Cycle 2: April Year 2 – October Year 3, which captures winter rainy seasons, such as are prevalent south of the equator.

Figure 4. Phenology metrics using the threshold method, indicating the start of season (SOS), length of season (LOS), date of maximum NDVI of the season (maxNDVI), and the cumulated NDVI over the season (cumNDVI).

A.

PDO_MAM_SOS1

B.

PDO_MAM_SOS1

-1.00 - -0.82	0.09 - 0.27
-0.82 - -0.64	0.27 - 0.45
-0.64 - -0.45	0.45 - 0.64
-0.45 - -0.27	0.64 - 0.82
-0.27 - -0.09	0.82 - 1.00

0.000 - 0.025
0.025 - 0.050
0.050 - 0.100
0.100 - 0.200
0.200 - 1.000
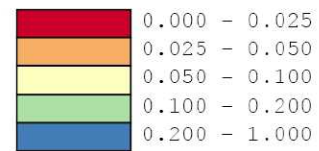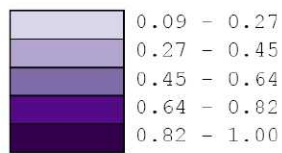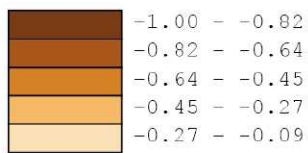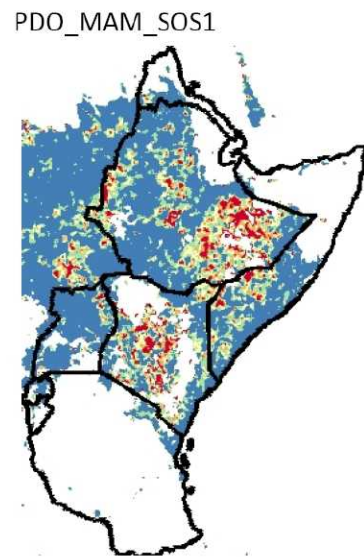
Figure 5. A. Image shows the correlation between the Pacific Decadal Oscillation during the March-April-May period on the start of season metric derived from NDVI from 1981-2007 in Eastern Africa. Note the differential effect in central Ethiopia where the high elevation areas are located. B. shows the significance (p value) of A. Brown colors in A. refer to earlier start times, blue colors to later start times.
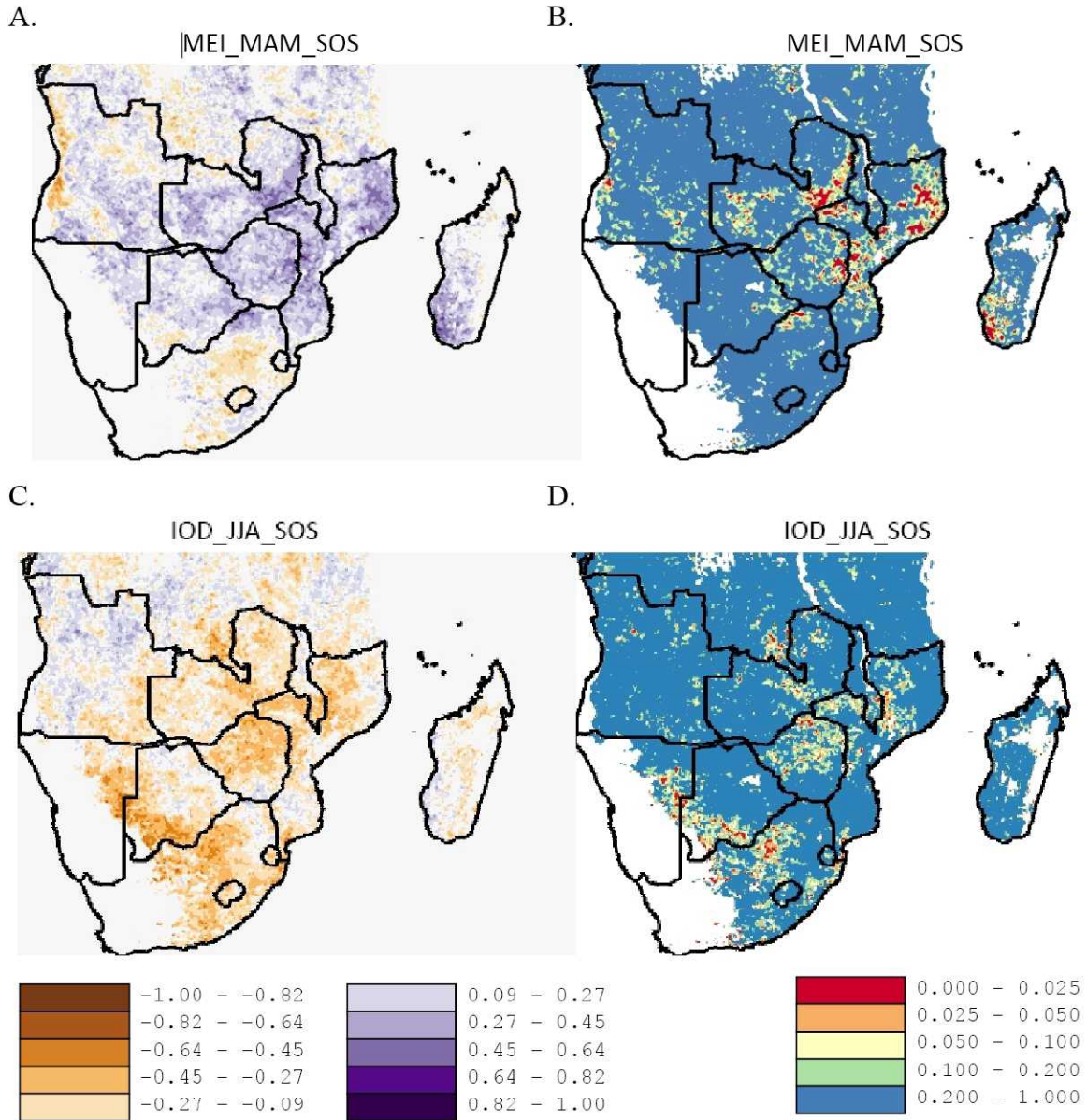
Figure 6. A. Correlation between the MEI from March-April-May (MAM) and start of season (SOS), B. shows the significance (p value) of A, C. Correlation between the IOD from June-July-August (JJA) on SOS in southern Africa, D. Significance of the correlation shown in C. Brown colors in the correlation refer to earlier start times, blue colors to later start times.
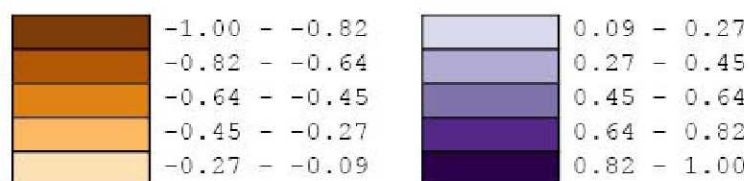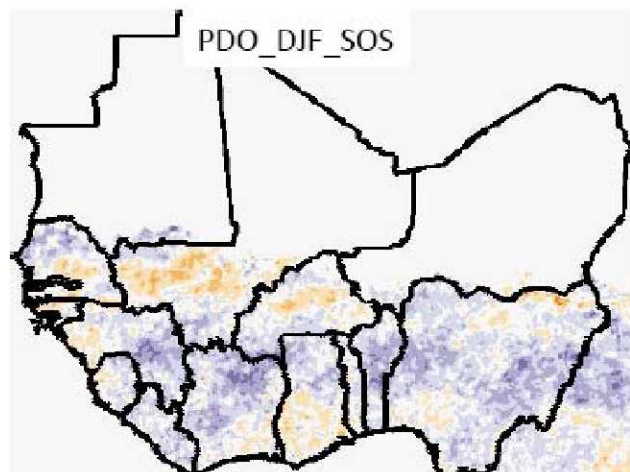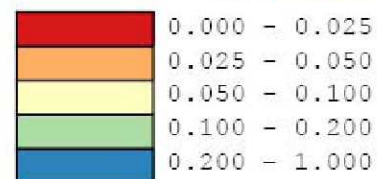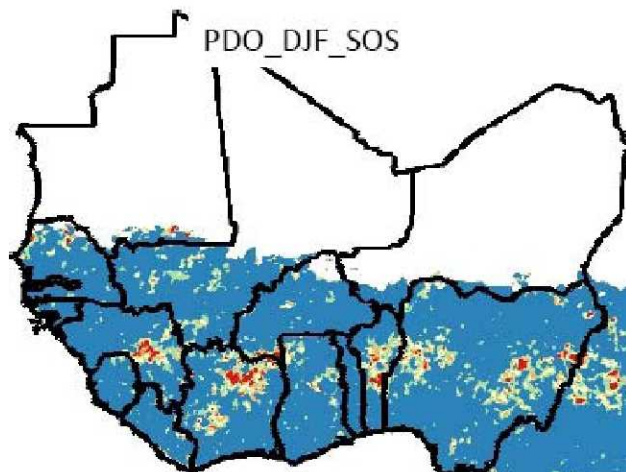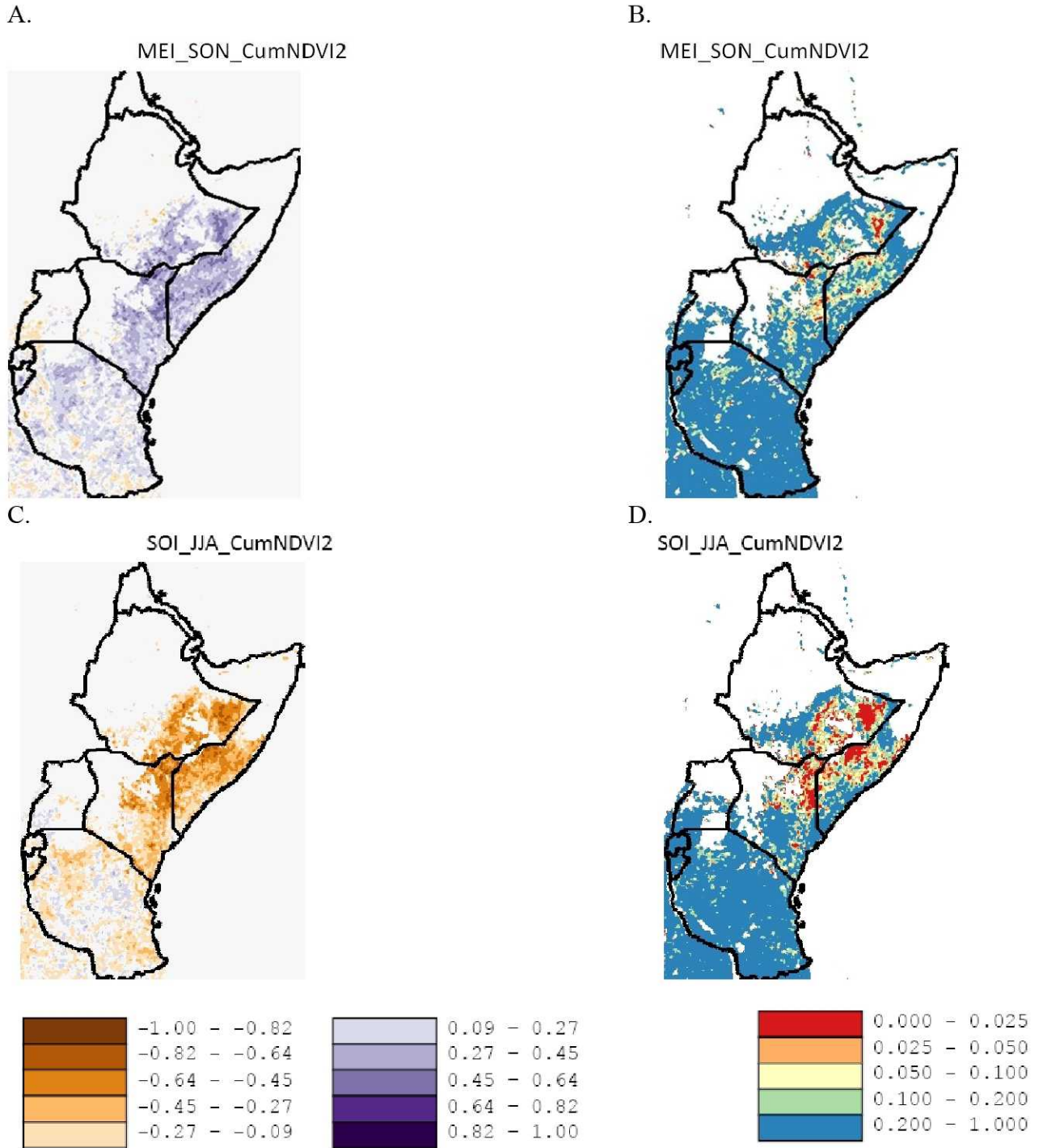
Figure 7. A. Correlation between the PDO from December-January-February (DJF) and start of season, B. shows the significance (p value) of the correlation in Western Africa. Brown colors in A correlate to earlier start times, blue colors to later start times.

Figure 8. A. Correlation between the MEI from September-October-November and cumulative NDVI, B. shows the significance (p value) of A, C. Correlation between the SOI from June-July-August (JJA) on cumulative NDVI, D. Significance of the correlation shown in C. Brown colors correlate to earlier start times, blue colors to later start times.
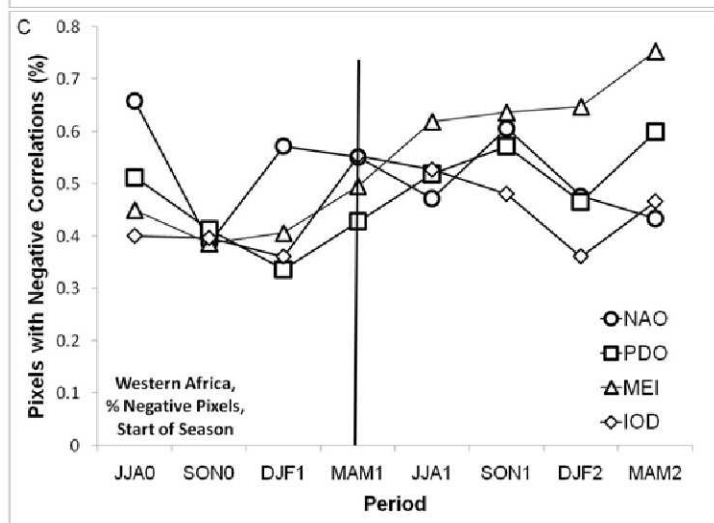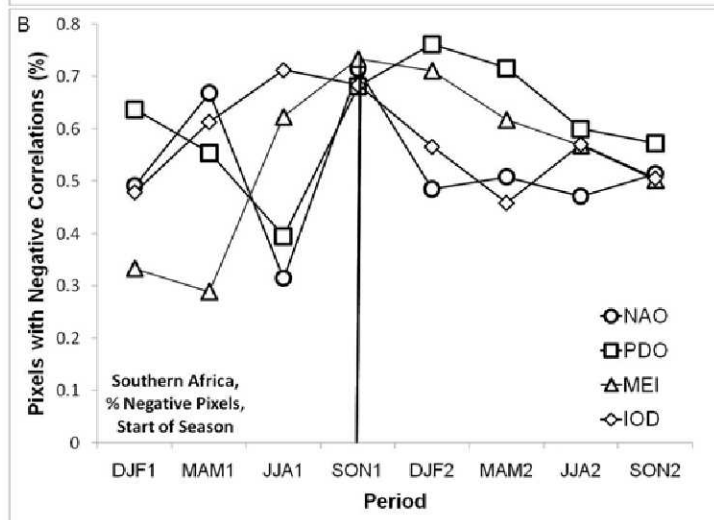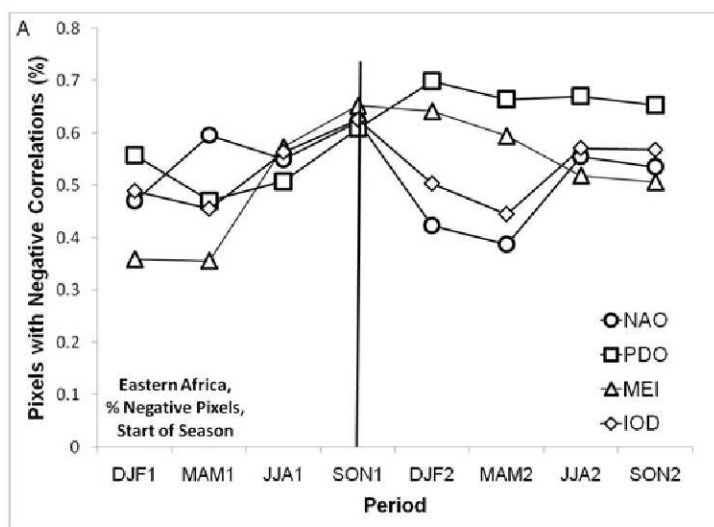
Figure 9. Analysis of the negative impact of four climate indices (NAO, PDO, MEI and IOD) on SOS for the three regions Eastern Africa (A), Southern Africa (B) and Western Africa (C). The black vertical lines correspond to the period when on average SOS occurs
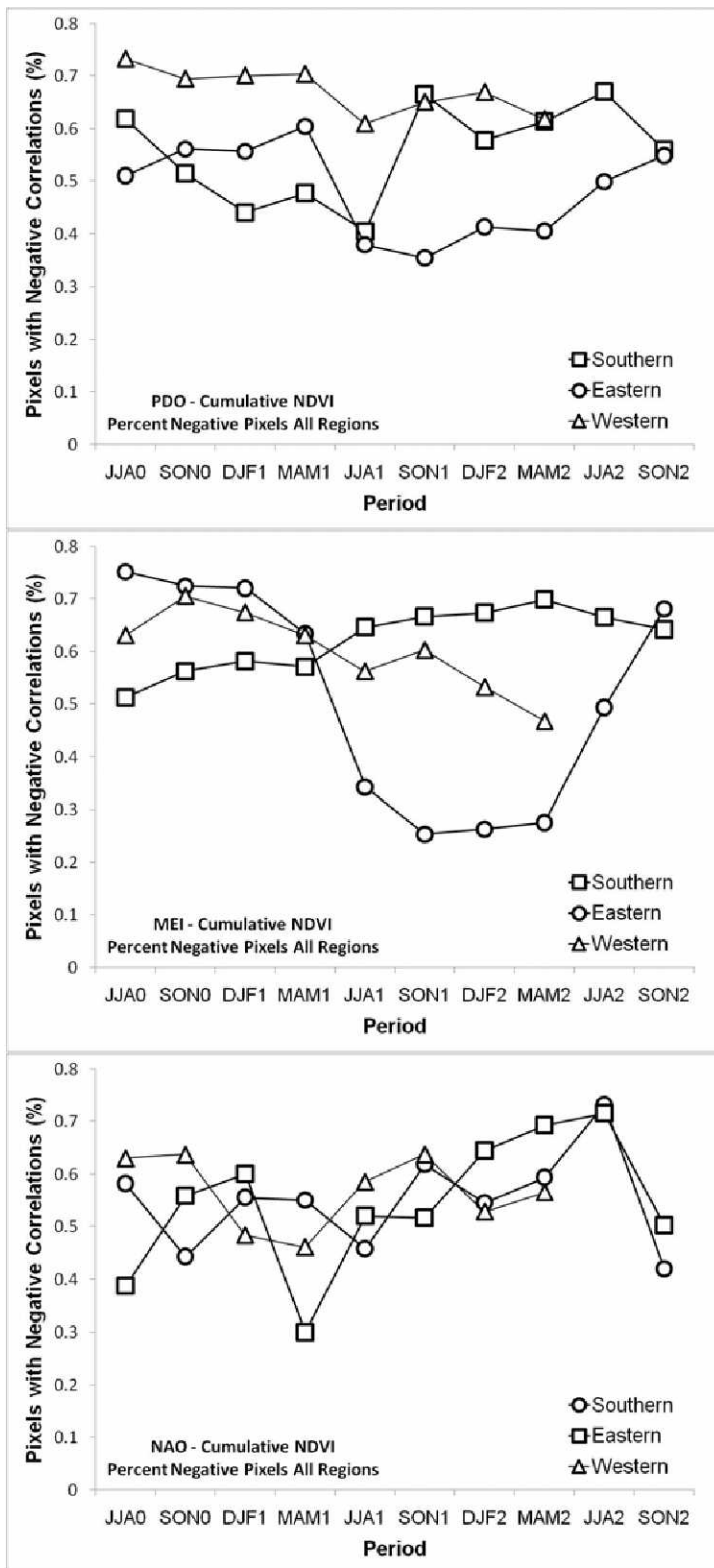
Figure 10. PDO, MEI and NAO effects by percent of region on cumulative NDVI.

References

Alberts, B., & Mehta, G. (2004). *Realizing the Promise and Potential of African Agriculture*. Amsterdam, The Netherlands: Interacademy Council

Anyamba, A. (1997). Interannual Variations of NDVI over Africa and their Relationship to ENSO: 1982-1995. In, *Department of Geography* (p. 132): Clark University

Anyamba, A., Tucker, C.J., & Eastman, J.R. (2001). NDVI anomaly patterns over Africa during the 1997/1998 ENSO warm event. *International Journal of Remote Sensing, 22*, 1847-1859

Bonan, G. (2002). *Ecological Climatology*. London: Cambridge University Press

Breman, H. (2003). West Africa's Subsistence Farming. In (p. 16). Togo: Food and Agriculture Organization, Rome

Brown, M.E. (2008a). *Famine Early Warning Systems and Remote Sensing Data*. Heildelberg: Springer Verlag

Brown, M.E. (2008b). *Famine Early Warning Systems and Remote Sensing Data*. Heidelberg: Springer Verlag

Brown, M.E., & De Beurs, K.M. (2008). Evaluation of Multi-Sensor Semi-Arid Crop Season Parameters Based on NDVI and Rainfall. *Remote Sensing of Environment, 112*, 2261-2271

Brown, M.E., Funk, C., Galu, G., & Choularton, R. (2007). Earlier Famine Warning Possible Using Remote Sensing and Models. *EOS Transactions of the American Geophysical Union, 88*, 381-382

Brown, M.E., Pinzon, J.E., & Prince, S.D. (2006). The Sensitivity of Millet Prices to Vegetation Dynamics in the Informal Markets of Mali, Burkina Faso and Niger. *Climatic Change, 78*, 181-202

Cane, M.A., Clement, A., Kaplan, A., Kushnir, Y., Pozdnyakov, D., Seager, R., Zebiak, S.E., & Murtugudde, R. (1996). 20th-Century Sea-Surface Temperature Trends. *Science, 275*, 957-960

Chen, J., Jönsson, P., Tamura, M., Gu, Z., Matsushita, B., & Eklundh, L. (2004). A simple method for reconstructing a high-quality NDVI time-series data set based on the Savitzky-Golay filter. *Remote Sensing of Environment, 91*, 332-344

Chen, X.Q., Tan, Z.J., Schwartz, M.D., & Xu, C.X. (2000). Determining the growing season of land vegetation on the basis of plant phenology and satellite data in Northern China. *International Journal of Biometeorology, 44*, 97-101

Chuvieco, E. (1999). Measuring changes in landscape pattern from satellite images: short-term effects of fire on spatial diversity. *International Journal of Remote Sensing, 20*, 2331-2346

de Beurs, K.M., & Henebry, G.M. (2008). Northern Annular Mode effects on the Land Surface Phenologies of Northern Eurasia. *Journal of Climate, 21*, 4257-4279

Eastman, J.R., Anyamba, A., & Ramachandran, M. (1996). The Spatial Manifestations of ENSO Warm Phase Events in Southern Africa. In, *Conference on the Application of Remotely Sensed Data and Geographic Information Systems in Environmental and Natural Resources Assessment in Africa*. Harare, Zimbabwe

FAO (2006). The State of Food Insecurity in the World. In (p. 30). Rome, Italy: United Nations Food and Agriculture Organization

FEWS (1992). Determining Start of the Growing Season using Max NDVI. In (p. 18). Arlington, VA: FEWS-ARD

FEWS (2008). Food Price Database at USGS Africa Data Dissemination Service (ADDS). In: USAID

FEWSNET (2006). KENYA FOOD SECURITY UPDATE – DECEMBER 6, 2006. In (p. 5). Washington DC: Famine Early Warning System Network

Fontaine, B., Trzaska, S., & Janicot, S. (1998). Evolution of the Relationship between near Global and Atlantic SST Modes and the Rainy Season in West Africa: Statistical Analyses and Sensitivity Experiments. *Climate Dynamics, 14*, 353-368

Funk, C., & Budde, M. (2008). Phenologically-tuned MODIS NDVI-based production anomaly estimates for Zimbabwe. *Remote Sensing of Environment, accepted*

Funk, C., Dettinger, M.D., Michaelsen, J.C., Verdin, J.P., Brown, M.E., Barlow, M., & Hoell, A. (2008). Warming of the Indian Ocean threatens eastern and southern African food security but could be mitigated by agricultural development. *Proceedings of the National Academy of Science, 105*, 11081-11086

Funk, C., Sanay, G., Asfaw, A., Korecha, D., Choularton, R., Verdin, J., Eilerts, G., & Michaelsen, J. (2005). Recent Drought Tendencies in Ethiopia and Equatorial-Subtropical Eastern Africa. In (p. 11). Washington DC: Famine Early Warning System Network, USAID

Glantz, M.H., Katz, R.W., & Nicholls, N. (1991). *Teleconnections Linking World Wide Climate Anomalies: Scientific Basis and Societal Impact*. New York: Cambridge University Press

Green, R.M., & Hay, S.I. (2002). The potential of Pathfinder AVHRR data for providing surrogate climatic variables across Africa and Europe for epidemiological applications. *Remote Sensing of Environment, 79*, 166-175

Groten, S.M.E., & Ocatre, R. (2002). Monitoring the length of the growing season with NOAA. *International Journal of Remote Sensing, 24*, 2797-2815

Holben, B. (1986). Characteristics of Maximum-Value Composite Images from Temporal AVHRR Data. *International Journal of Remote Sensing, 7*, 1417-1434

Hurrell, J.W. (1995). Decadal trends in the North Atlantic Oscillation: Regional temperatures and precipitation. *Science, 269*, 676-679

Ji, L., & Peters, A.J. (2003). Assessing vegetation response to drought in the northern Great Plains using vegetation and drought indices. *Remote Sensing of Environment, 87*, 85-98

Jones, P.D., Jónsson, T., & Wheeler, D. (1997). Extension to the North Atlantic Oscillation using early instrumental pressure observations from Gibraltar and South-West Iceland. *International Journal of Climatology, 17*, 1433-1450

Jury, M.R., McQueen, C., & Levey, K. (1994). SO1 and QBO Signals in the African Region. *Theoretical and Applied Climatology, 50*, 103-115

Lehman, E.L., & D'Abrera, H.J.M. (1975). *Nonpara-metrics-Statistical Methods Based on Ranks*. San Francisco,CA: Holden-Day

Mabaso, M., Kleinschmidt, I., Sharp, B., & Smith, T. (2009). El Niño Southern Oscillation (ENSO) and annual malaria incidence in Southern Africa. *Transactions of the Royal Society of Tropical Medicine and Hygiene, 101*, 326-330

Mantua, N.J., Hare, S.R., Zhang, Y., Wallace, J.M., & Francis, R.C. (1997). A Pacific interdecadal climate oscillation with impacts on salmon production. *Bulletin of the American Meteorological Society, 78*, 1069-1079

Nicholson, S. (2003). The South Indian Convergence Zone and Interannual Rainfall Variability over Southern Africa and the Question of ENSO's Influence on Southern Africa. *Journal of Climate, 16*, 555-562

Parry, M.L., Canziani, O.F., Palutikof, J.P., Linden, P.J.v.d., & Hanson, C.E. (Eds.) (2007). *IPCC, 2007: Climate Change 2007: Impacts, Adaptation and Vulnerability. Contribution of Working Group II to the Fourth Assessment Report of the Intergovernmental Panel on Climate Change*. Cambridge, UK: Cambridge University Press

Pinzon, J., Brown, M.E., & Tucker, C.J. (2005). Satellite time series correction of orbital drift artifacts using empirical mode decomposition. In N. Huang (Ed.), *Hilbert-Huang Transform: Introduction and Applications* (pp. 167-186)

Rasmussen, E. (1991). Observational aspects of ENSO cycle teleconnections. In R.W.K. M. H. Glantz, and N. Nicholls (Ed.), *Teleconnections Linking Worldwide Climate Anomalies* (pp. 309-344): Cambridge University Press

Rasmussen, M.S. (1998). Developing simple, operational, consistent NDVI-vegetation models by applying environmental and climatic information. Part I: Assessment of net primary production. *International Journal of Remote Sensing, 19*, 97-119

Rasmusson, E.M., & Wallace, J.M. (1983). Meteorological aspects of the El Niño/Southern Oscillation. *Science, 222*, 1195-1202

Reason, C.J.C., & Rouault, M. (2002). ENSO-like decadal variability and South African rainfall. *Geophysical Research Letters, 29*, 10.1029/ 2002GL014663, 014616-014661-014664

Reynolds, R.W., Rayner, N.A., Smith, T.M., Stokes, D.C., & Wang, W. (2002). An Improved In Situ and Satellite SST Analysis for Climate. *Journal of Climate, 15*, 1609-1625

Ropelewski, C.F., & Halpert, M.S. (1986). Global and Regional Scale Precipitation Patterns Associated with the El Nino/Southern Oscillation. *Monthly Weather Review, 115*, 1606-1626

Ropelewski, C.F., & Halpert, M.S. (1987). Global and Regional Scale Precipitation Patterns Associated with the El Nino/Southern Oscillation. *Monthly Weather Review, 115*, 1606-1626

Saji, N., Goswami, B., & Yamagata, T. (1999). A dipole mode in the tropical Indian Ocean. *Nature, 401*, 360-363

Thompson, D.W., & Wallace, J.M. (2001). Regional climate impacts of the Northern Hemisphere Annular Mode. *Science, 293*, 85-89

Tucker, C.J., Pinzon, J.E., Brown, M.E., Slayback, D., Pak, E.W., Mahoney, R., Vermote, E., & Saleous, N. (2005). An Extended AVHRR 8-km NDVI Data Set Compatible with MODIS and SPOT Vegetation NDVI Data. *International Journal of Remote Sensing, 26*, 4485-4498

UCAR (2009). Persistent Patterns that Shape Weather and Climate Variability—A Glossary. In B.H. Kevin Trenberth, Zhenya Gallon (Ed.), *Backgrounders*. Boulder, CO: NCAR/UCAR

USAID (2007). The History of America's Food Aid. In: US State Department

Vasagar, J. (2005). Plenty of Food - Yet the Poor are Starving. In, *Guardian (UK)*. TAHOUA, Niger

Verdin, J., Funk, C., Kalver, R., & Roberts, D. (1999). Exploring the correlation between Southern Africa NDVI and Pacific sea surface temperatures: results for the 1998 Maize growing season. *International Journal of Remote Sensing, 20*, 2117-2124

Verdin, J., Lietzow, R., Rowland, J., Klaver, R., Reed, B., French, V., & Lee, F. (2000). A Comparison Of Methods For Estimating Start-Of-Season From Operational Remote Sensing Products: First Results. In (p. 13). Sioux Falls, SD: USGS-EROS Data Center

Vrieling, A., De Beurs, K.M., & Brown, M.E. (2008). Recent trends in agricultural production of Africa based on AVHRR NDVI time series. In, *SPIE Europe Security + Defense*. Cardiff, UK

Wang, G. (2003). Reassessing the impact of North Atlantic Oscillation on the sub-Saharan vegetation production. *Global Change Biology, 9*, 493-499

White, M.A., Thornton, P.E., & Running, S.W. (1997). A continental phenology model for monitoring vegetation responses to interannual climatic variability. *Global Biogeochemical Cycles, 11*, 217-234

Wolter, K., & Timlin, M.S. (1998). Measuring the strength of ENSO - how does 1997/98 rank? *Weather, 53*, 315-324

Zhang, R., & Delworth, T.L. (2006). Impact of Atlantic multidecadal oscillations on India/Sahel rainfall and Atlantic hurricanes. *Geophysical Research Letters, 33*, doi:10.1029/2006GL026267